Journal of
Synchrotron Radiation

ISSN 0909-0495

addenda and errata

Calcifications in human osteoarthritic articular cartilage: e*x vivo* assessment of calcium compounds using XANES spectroscopy. Addendum

Christelle Nguyen,[a,b] Hang Korng Ea,[a,b,c] Dominique Thiaudiere,[d] Solenn Reguer,[d] Didier Hannouche,[e,f] Michel Daudon,[g,h] Frédéric Lioté[a,b,c] and Dominique Bazin[i]*

[a]UMR-S 606, INSERM, Lariboisière Hospital, Paris, France, [b]Paris Diderot University, Paris, France, [c]Rheumatology Department, Centre Viggo Petersen, Pôle Appareil Locomoteur, Lariboisière Hospital, Assistance Publique-Hôpitaux de Paris (AP-HP), Paris, France, [d]Synchrotron SOLEIL, L'Orme des Merisiers, Saint-Aubin, BP 48, 91192 Gif-sur-Yvette, France, [e]Orthopaedic Surgery Department, Pôle Appareil Locomoteur, Lariboisière Hospital, Paris, France, [f]CNRS UMR 7052, Paris Diderot University, Paris, France, [g]Service de Biochimie A, Necker Hospital (AP-HP), Paris, France, [h]Paris Sud University, Paris, France, and [i]Laboratoire de Physique des Solides, Paris Sud University, Orsay, France. E-mail: bazin@lps.u-psud.fr

An acknowledgment is published for the paper by Nguyen *et al.* [(2011), *J. Synchrotron Rad.* **18**, 475–480].

The authors of Nguyen *et al.* (2011) would like to add the following acknowledgment: Additionnal fundings were received from the Fondation pour la Recherche Médicale (appel 'Vieillissement Ostéoarticulaire'), ARPS and Association Rhumatisme et Travail.

References

Nguyen, C., Ea, H. K., Thiaudiere, D., Reguer, S., Hannouche, D., Daudon, M., Lioté, F. & Bazin, D. (2011). *J. Synchrotron Rad.* **18**, 475–480.

 doi:10.1107/S090904951101689X

Journal of
Synchrotron Radiation

ISSN 0909-0495

Received 8 December 2010
Accepted 23 February 2011

Calcifications in human osteoarthritic articular cartilage: *ex vivo* assessment of calcium compounds using XANES spectroscopy

Christelle Nguyen,[a,b] Hang Korng Ea,[a,b,c] Dominique Thiaudiere,[d] Solenn Reguer,[d] Didier Hannouche,[e,f] Michel Daudon,[g,h] Frédéric Lioté[a,b,c] and Dominique Bazin[i]*

[a]UMR-S 606, INSERM, Lariboisière Hospital, Paris, France, [b]Paris Diderot University, Paris, France, [c]Rheumatology Department, Centre Viggo Petersen, Pôle Appareil Locomoteur, Lariboisière Hospital, Assistance Publique-Hôpitaux de Paris (AP-HP), Paris, France, [d]Synchrotron SOLEIL, L'Orme des Merisiers, Saint-Aubin, BP 48, 91192 Gif-sur-Yvette, France, [e]Orthopaedic Surgery Department, Pôle Appareil Locomoteur, Lariboisière Hospital, Paris, France, [f]CNRS UMR 7052, Paris Diderot University, Paris, France, [g]Service de Biochimie A, Necker Hospital (AP-HP), Paris, France, [h]Paris Sud University, Paris, France, and [i]Laboratoire de Physique des Solides, Paris Sud University, Orsay, France. E-mail: bazin@lps.u-psud.fr

Calcium (Ca^{2+})-containing crystals (CCs), including basic Ca^{2+} phosphate (BCP) and Ca^{2+} pyrophosphate dihydrate (CPPD) crystals, are associated with severe forms of osteoarthritis (OA). Growing evidence supports a role for abnormal articular cartilage mineralization in the pathogenesis of OA. However, the role of Ca^{2+} compounds in this mineralization process remains poorly understood. Six patients, who underwent total knee joint replacement for primary OA, have been considered in this study. Cartilage from femoral condyles and tibial plateaus in the medial and lateral compartments was collected as 1 mm-thick slices cut tangentially to the articular surface. First, CCs presence and biochemical composition were assessed using Fourier transform infrared spectroscopy (FT-IR). Next, Ca^{2+} compound biochemical form was further assessed using X-ray absorption spectroscopy (XAS) performed at the Ca^{2+} *K*-absorption edge. Overall, 12 cartilage samples were assessed. Using FT-IR, BCP and CPPD crystals were detected in four and three out of 12 samples, respectively. Ca^{2+} compound biochemical forms differed between areas with *versus* without CCs, when compared using XAS. The complete set of data shows that XANES spectroscopy can be used to accurately characterize sparse CCs in human OA cartilage. It is found that Ca^{2+} compounds differ between calcified and non-calcified cartilage areas. In calcified areas they appear to be mainly involved in calcifications, namely Ca^{2+} crystals.

Keywords: calcium-containing crystals; cartilage; osteoarthritis; Fourier-transform infrared spectroscopy; X-ray absorption spectroscopy.

1. Introduction

Osteoarthritis (OA) affects the entire joint. Thus, in addition to articular cartilage destruction, OA induces changes in other joint components including the bone, menisci, synovium, ligaments, capsule and muscles (Hunter & Felson, 2006). Multiple factors including the genetic background, mechanical overload, ageing and intra-articular calcium (Ca^{2+})-containing microcrystal (CC) deposition contribute to the pathogenesis and progression of OA. CCs encountered in human crystal deposition-associated joint diseases include Ca^{2+} pyrophosphate dihydrate (CPPD) and basic Ca^{2+} phosphate (BCP) crystals. CPPD crystals ($Ca_2P_2O_7{\cdot}2H_2O$) are found as triclinic and/or monoclinic forms (t-CPPD and m-CPPD, respectively) (Mandel & Mandel, 1988). BCP crystals encompass octacalcium phosphate [OCP; $Ca_8(HPO_4)_2(PO_4)_4{\cdot}5H_2O$], carbonated apatite [CA; $Ca_{10}(PO_4)_6(OH)_x(CO_3)_y$], tricalcium phosphate [$Ca_3(PO_4)_2$] (McCarty *et al.*, 1983) and magnesium whitlockite (Scotchford & Ali, 1995) crystals. A pathogenic role for CC-associated microcrystalline stress in OA is supported by recent clinical and experimental findings (Ea *et al.*, 2011; Nguyen *et al.*, 2010). CCs have been identified in 60% of OA synovial fluids and in 100% of OA cartilages obtained during total knee or hip joint replacement (Derfus *et al.*, 2002; Fuerst, Bertrand *et al.*, 2009; Fuerst, Niggemeyer *et al.*, 2009). CCs are associated with destructive forms of OA, as well as with chondrocyte differentiation toward a pro-mineralizing phenotype (Fuerst, Bertrand *et al.*, 2009). *In vitro*, CCs can

activate various cell types by several mechanisms and display mitogenic, catabolic, inflammatory and apoptotic properties (Ea & Lioté, 2009; McCarthy & Cheung, 2009). *In vivo*, their presence can precede cartilage breakdown (Bendele & Hulman, 1988; Evans *et al.*, 1994), and intra-articular injection of CPPD crystals worsens rabbit OA lesions induced by anterior cruciate ligament section (Fam *et al.*, 1995).

The mechanisms underlying articular cartilage mineralization during OA are incompletely understood. Briefly, calcification can occur when the balance between inhibitors and pro-mineralizing factors is disrupted by any of multiple influences such as genetics, ageing, extracellular matrix modifications, dysregulation of inorganic pyrophosphate (PPi) and phosphate (Pi) metabolisms, changes in extracellular Ca^{2+} levels, and chondrocyte phenotype alterations (Ea & Lioté, 2009). Cartilage calcifications are formed at least partly in chondrocyte-derived apoptotic bodies (Johnson *et al.*, 2001) and matrix vesicles (MVs), which are membrane-enclosed particles released from the plasma membrane of mineralization-competent cells (Anderson, 1995). Apatite crystal formation within MVs in OA cartilage has been documented by electron microscopy (Kirsch *et al.*, 2000). Concentrations of Ca^{2+} (30–50 mmol l^{-1}) and inorganic phosphate (Pi) (15–30 mmol l^{-1}) in MVs are well above the minimum level of [Ca]·[Pi] supersaturation, at which amorphous Ca^{2+} phosphate, considered a precursor of biological apatite, spontaneously precipitates at physiological pH (Termine & Eanes, 1974). Ca^{2+} binding to proteins and lipids within the MV lumen, together with an imbalance between Pi and PPi (Camerlain *et al.*, 1975; Terkeltaub, 2001), is among the driving forces of early mineral ion uptake (Sauer & Wuthier, 1988) and ultimately leads to tissue mineralization. Compared with normal cartilage, OA cartilage consistently showed increased Ca^{2+} and Pi contents, of 128.9 mmol kg^{-1} *versus* 52.6 mmol kg^{-1} for Ca^{2+} and 66.9 mmol kg^{-1} *versus* 23.1 mmol kg^{-1} for Pi (Pritzker *et al.*, 1987). Increased extracellular Ca^{2+} drives chondrocyte differentiation toward a pro-mineralizing phenotype (Bonen & Schmid, 1991), whereas extracellular Ca^{2+} depletion maintains a stable cellular phenotype (Gigout *et al.*, 2005). However, little is known regarding the state of Ca^{2+} compounds in human OA articular cartilage.

Accurate characterization of calcifications is difficult to achieve using conventional techniques available in clinical laboratories. Among the techniques that are often used to characterize calcifications, diffraction techniques (using neutrons, X-rays or electrons as probes) (Guinier, 1956) and vibrational spectroscopy [including Raman and Fourier transform infrared (FT-IR) spectroscopy] (Kneipp *et al.*, 1999; McKelvy *et al.*, 1998) are very effective tools for studying mineralized tissues. Recent experimental developments permit *ex vivo* and *in vivo* experiments at the micrometre scale (Bertsch & Hunter, 2001; Dumas *et al.*, 2006). Physico-chemical techniques available for the structural characterization of cartilage and other biological samples include techniques specific to large instruments (Bazin *et al.*, 2006), such as synchrotron radiation X-ray fluorescence (Bazin *et al.*, 2007; Zoeger *et al.*, 2006), X-ray diffraction (Yarker *et al.*, 1984) and X-ray absorption spectroscopy (XAS) (Eichert *et al.*, 2005). XAS is a sensitive technique, specific to synchrotron radiation, which has been used to characterize the local environment of specific elements such as Ca^{2+} and Zn^{2+} in biological samples. Measurements can be performed directly on the sample with minimal preparation (Bazin *et al.*, 2009*a*,*b*; Carpentier *et al.*, 2010). XAS techniques include X-ray absorption near-edge structure spectroscopy (XANES) and extended X-ray absorption fine-structure spectroscopy (Eichert *et al.*, 2005; Sowrey *et al.*, 2004) and provide an accurate description of the electronic state, geometry of very first neighbours, and first coordination spheres of the selected element.

The objective of this study was to use XAS performed at the Ca^{2+} *K*-absorption edge (XANES) to compare the state of Ca^{2+} compounds between human OA articular cartilage areas with CCs *versus* areas without CCs.

2. Experimental design

2.1. Patients

Specimens of knee joint cartilage were obtained from six patients undergoing total knee replacement surgery for OA at a single orthopaedic department. Patients were selected at random and included prospectively. One rheumatologist (CN) reviewed the medical file of each patient. Clinical data [age; sex; body mass index (BMI); and presence of genu varum or genu valgum] and preoperative plain knee radiographs were obtained and analysed. Kellgren and Lawrence staging was used to characterize OA severity. Patients with secondary OA (inflammatory disease or trauma) were not included.

2.2. Cartilage sample preparation

Specimens included femoral condyle and tibial plateau cartilages from both the medial and the lateral compartments (Fig. 1*a*), yielding a theoretical total of eight cartilage zones per knee. Specimens were washed three times with saline under aseptic conditions to avoid contamination by bone mineral crystals released at the time of surgery. For each femoro-tibial compartment, samples were collected as 1 mm-thick slices cut with a scalpel tangentially to the articular cartilage surface. Cartilage areas were labelled as follows: 1, medial condyle; 2, lateral condyle; 3, medial tibial plateau; 4, lateral tibial plateau; S, superficial layer; and D, deep layer (Fig. 1*b*). Cartilage samples were either frozen directly and stored at 253 K for FT-IR or fixed in 70° alcohol at 277 K for XAS. This protocol was used in order to preserve the physico-chemical integrity of the mineral part of the samples. Of note, preservation of the balance between intra- and extra-cellular ions such as Ca^{2+} requires a different and specific preparation protocol (Boxer *et al.*, 2009).

2.3. Fourier transform infrared (FT-IR) spectroscopy

Cartilage samples were first characterized using FT-IR spectrometry (Vector 22; Brucker Spectrospin, Wissembourg, France) as previously described (Estepa & Daudon, 1997). Data were collected in the absorption mode between 4000 and

400 cm^{-1}, with a resolution of 4 cm^{-1}. The absorption bands of Ca^{2+} biological reference compounds, namely CA, amorphous Ca^{2+} carbonated phosphate (ACCP) and CPPD, are well documented. Regarding CA, the ν_1 and ν_3 P—O stretching vibration modes are measured at 960–962 cm^{-1} and 1035–1045 cm^{-1}, respectively, while the O—P—O ν_4 bending mode corresponds to the doublet at 602–563 cm^{-1}. The bands at 3570 and 633 cm^{-1}, corresponding to the stretching and vibrational modes of the OH— groups characteristic of hydroxyapatite, are absent from CA. Disappearance of the CA shoulder in the ν_3 absorption band is a fingerprint for ACCP. Regarding m-CPPD, O—P—O bending is recorded at 535 cm^{-1} and 508 cm^{-1}. P—O stretching vibrations generate absorptions at 923 cm^{-1} and 991 cm^{-1}, whereas asymmetric stretching vibrations give rise to absorptions at 1037 cm^{-1} and 1089 cm^{-1}.

2.4. X-ray absorption spectroscopy

Experiments were performed at room temperature and atmospheric pressure, on the DIFFABS beamline located at the D13-1 bending magnet at the SOLEIL synchrotron facility (Saint Aubain, France). The typical energy of the storage ring was 2.75 GeV with an average current of 300 mA in the new TOP/UP configuration. Monochromatization and horizontal focus were achieved using a double Si (111) crystal monochromator that provided an energy resolution of $\Delta E/E = 10^{-4}$, which was necessary for XANES resolution. The monochromator was positioned between two cylindrical vertically focusing mirrors (50 nm Rh deposited on Si substrates). At the position of the sample, spot size was defined using slits to reach 100 µm × 250 µm (H × V, FWHM). Spectra at the Ca *K*-absorption edge (4086 eV) were collected in the 4020–4140 eV energy range, with energy steps of 0.5 eV and a 3 s dwell time per point. At least four different areas of each sample were analysed. Additional details on the experimental set-up have been reported previously (Carpentier *et al.*, 2010).

Table 1
Demographic, clinical and osteoarthritis features in the six patients with knee osteoarthritis.

Data are number (%), unless otherwise indicated. SD, standard deviation; OA, osteoarthritis.

Age in years, mean (SD)	74 (9)
Male gender	1
Body mass index, kg m^{-2}, mean (SD)	28 (9)
Genu varum	5 (83)
Kellgren, mean (SD)	4 (0)
Unicompartmental OA	1 (17)
Bicompartmental OA	3 (50)
Tricompartmental OA	2 (33)
OA mainly affecting the medial femoro-tibial compartment	6 (100)
Preoperative radiographic calcifications	1 (17)
Calcifications by macroscopic examination	6 (100)
Calcifications by microscopic examination	6 (100)

2.5. Ethical considerations

All human sample collection procedures complied with the Helsinki Declaration. According to French Law on human research (Law 2007-1110, article 1211-2), cartilage sample collection (surgical waste) was authorized unless opposition from patients; all patients were informed and gave oral consent. As quoted above, formal approval from an ethical committee and a written consent from the patients are not required for studies using surgical waste materials.

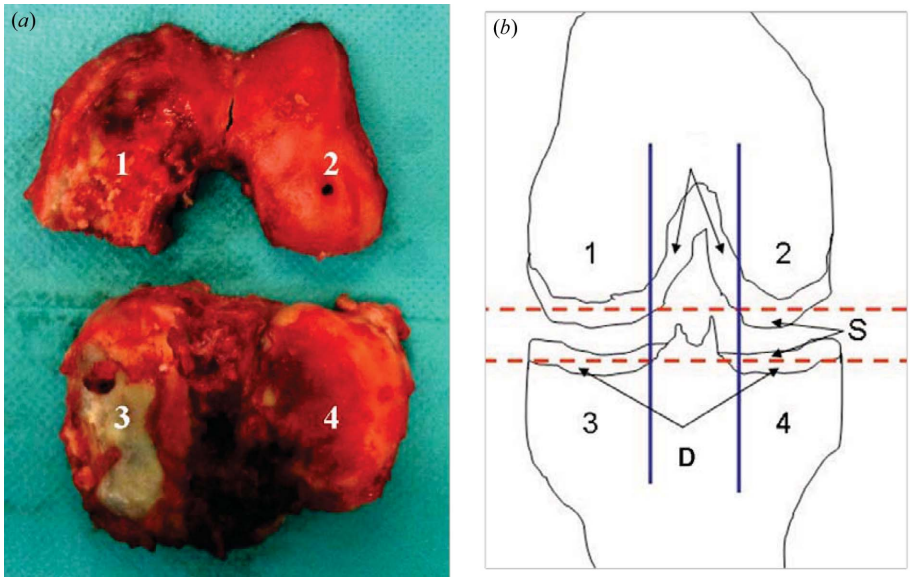

Figure 1
Knee joint specimen obtained during arthroplasty and schematic representation of the sample collection protocol. The specimen included femoral condyle and tibial plateau cartilage from both the medial and the lateral compartments (*a*). Cartilage areas were labelled as follows: 1, medial condyle; 2, lateral condyle; 3, medial tibial plateau; 4, lateral tibial plateau; S, superficial layer; D, deep layer (*b*).

3. Results

3.1. Clinical, demographic and OA characteristics

Overall, six patients (five females) were included. The mean (SD) age and body mass index at surgery were 74 (9) years (58 to 81 years) and 28 (9) kg m^{-2}, respectively. Preoperative plain radiographs showed uni-, bi- and tri-compartmental knee OA in 1, 3 and 2 patients, respectively. In all cases, OA was most severe in the medial femoro-tibial compartment, where the mean (SD) Kellgren and Lawrence score was 4 (0) (Table 1).

3.2. Identification and quantification of calcium-containing crystals in human OA articular cartilage using FT-IR

Although eight specimens per knee would have been obtained in theory, we only examined 12 specimens selected at random from the six patients and free of

Table 2
Identification and quantification of Ca^{2+}-containing crystals in 12 samples of osteoarthritis human articular cartilage using FT-IR spectroscopy.

Data are percentages. CA, carbonated apatite; CPPD, Ca^{2+}-pyrophosphate dihydrate; ACCP, amorphous carbonated Ca^{2+} phosphate; prot, proteins; TG, triglycerides; CH, carbohydrate. See §2 for explanations of sample labelling.

CA	CPPD	ACCP	Other (prot, TG, CH)	Total mineral phase	
0	0	0	100	0	XANES indicated Ca^{2+} in tissue
0	15	0	85	15	XANES indicated
0	15	0	85	15	Ca^{2+} in CPPD
10	0	0	90	10	XANES indicated
0	0	0	100	0	Ca^{2+} in tissue
0	0	0	100	0	XANES indicated
0	0	0	100	0	Ca^{2+} in tissue
5	0	0	95	5	XANES indicated
0	10	0	90	10	Ca^{2+} in tissue
0	0	0	100	0	XANES indicated
5	0	0	95	5	Ca^{2+} in tissue
5	0	0	95	5	

calcifications by macroscopic examination (Table 2) owing to limited XAS beam time. FT-IR showed CCs in at least one sample from four of the six patients. The main compounds identified were mixtures of proteins, triglycerides and carbohydrates. The total mineral phase accounted for 10% of the total sample on average. Two types of mineral phase were detected, CA and m-CPPD (in four and three samples, respectively) (Fig. 2). In five samples no mineral phase was detected (Table 2).

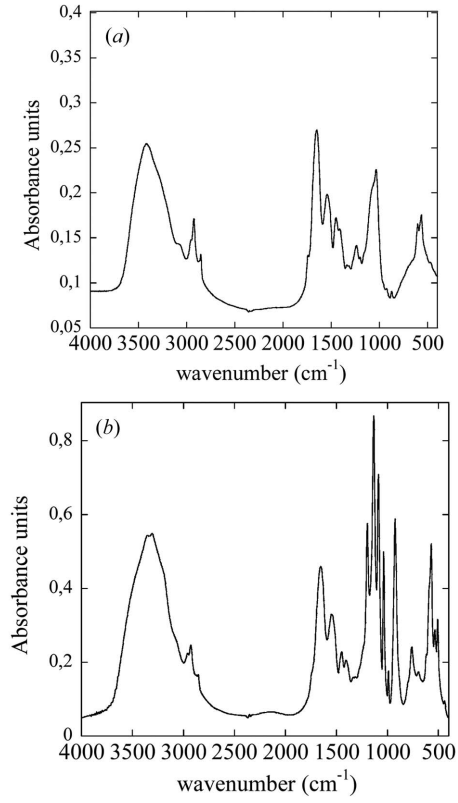

Figure 2
FT-IR absorption spectra representative of cartilage samples exhibiting calcium (Ca^{2+})-containing crystals (CC), namely, carbapatite (*a*) and Ca^{2+} pyrophosphate dehydrate crystals (*b*). The absorption bands of carbapatite (CA) and Ca^{2+} pyrophosphate dehydrate (CPPD) are well documented. Regarding CA, the ν_1 and ν_3 P—O stretching vibration modes are measured at 960–962 cm^{-1} and 1035–1045 cm^{-1}, respectively, while the O—P—O ν_4 bending mode corresponds to the doublet at 602–563 cm^{-1}. The bands at 3570 and 633 cm^{-1}, corresponding to the stretching and vibrational modes of the OH— groups characteristic of hydroxyapatite, are absent from CA. Regarding m-CPPD, O—P—O bending is recorded at 535 cm^{-1} and 508 cm^{-1}. P—O stretching vibrations correspond to absorptions at 923 cm^{-1} and 991 cm^{-1}, whereas asymmetric stretching vibrations give rise to absorptions at 1037 cm^{-1} and 1089 cm^{-1}.

3.3. XANES spectra of biological reference compounds

The three reference compounds used in this study and previously characterized by FT-IR analysis were one biological m-CPPD sample and two biological BCP samples, namely CA and ACCP. To obtain a signal corresponding to Ca^{2+} from the tissue, thus including both intra- and extracellular Ca^{2+}, we collected the XAS spectrum from cartilage areas with no calcifications by FT-IR (Fig. 3). After pre-peak A ascribable to a $1s \rightarrow 3d$ transition, the most intense transition resonance of the spectrum was observed. This structure included a shoulder-like feature (feature B, $1s \rightarrow 4s$ transition). For CA there was a double peak (features C1 and C2, $1s \rightarrow 4p$ transition), whose relative intensities depended on the type of Ca^{2+} involved [Ca(I) or Ca(II)]. For m-CPPD and ACCP a single peak was present. Of note, the peak corresponding to Ca^{2+} from the tissue displayed a higher intensity. In addition, the shape of the edge of the sample was very different from the shapes of the other reference compounds, suggesting that the XANES spectrum reflected Ca^{2+} atoms present in the tissue. For m-CPPD, an additional feature (D) was present at 4057 eV.

3.4. XANES spectra of human osteoarthritic articular cartilage compounds

Part of the sample was first analysed using FT-IR and the other part was investigated using XANES. In all five cartilage samples without CCs by FT-IR the XANES spectra were similar and displayed a large and very intense C peak corresponding to Ca^{2+} in the tissue. In patient 2, whose sample contained 15% of m-CPPD by FT-IR, the shape and position of the XANES spectrum were similar to those of the reference m-CPPD compound, whereas no tissue Ca^{2+} spectrum was detected (Fig. 4).

4. Discussion

Although the presence of CCs in osteoarthritic cartilage was recognized several decades ago, the relationship between CCs and OA remains controversial. Several recent studies support

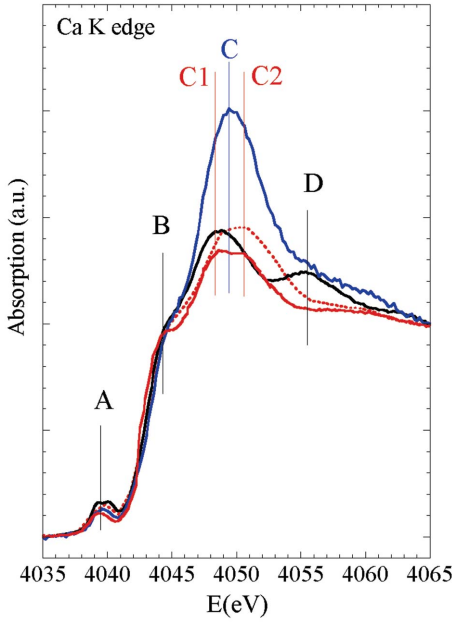

Figure 3
XANES spectra of reference compounds. Absorption spectra were obtained for biological cartilage samples previously characterized by FT-IR. Red solid line, carbapatite; red dotted line, amorphous carbonated Ca^{2+} apatite; black solid line, Ca^{2+} pyrophosphate dehydrate; blue solid line, non-diffusible tissue Ca^{2+}. Note the pre-peak A ($1s \rightarrow 3d$ transition), the shoulder B (transition $1s \rightarrow 4s$), the double peaks C1–C2 [$1s \rightarrow 4p$ transition, whose relative intensities depend on the type of Ca^{2+}, namely, Ca(I) or Ca(II) involved in apatite] and the single C peak for non-diffusible tissue Ca^{2+}.

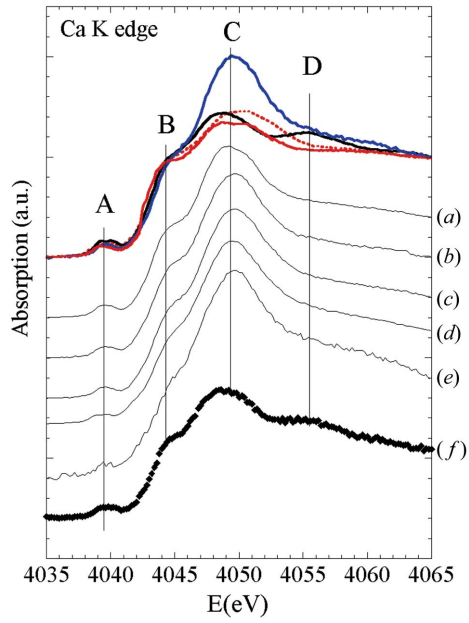

Figure 4
XANES human osteoarthritic articular cartilage compounds. Absorption spectra were obtained for biological cartilage samples previously characterized by FT-IR. Red solid line, carbapatite; red dotted line, amorphous carbonated Ca^{2+} apatite; black solid line, Ca^{2+} pyrophosphate dehydrate; blue solid line, non-diffusible tissue Ca^{2+}. (*a*) Patient 1. (*b*) Patient 3. (*c*) Patient 4. (*d*) Patient 5. (*e*) Patient 6. (*f*) Patient 2.

a pathogenic role for CCs in OA (Fuerst, Bertrand *et al.*, 2009; Fuerst, Niggemeyer *et al.*, 2009), thus confirming many earlier clinical and experimental studies, and suggest that articular cartilage mineralization may be a consistent feature of end-stage OA. However, the role for Ca^{2+} compounds in the mineralization process remains poorly understood. In the present study using XANES spectroscopy at the Ca^{2+} *K*-edge, a powerful technique specific to synchrotron radiation, we found differences in Ca^{2+} compound biochemical composition between cartilage areas with and without CCs from patients with end-stage OA. Thus, in areas without CCs, a specific XANES spectrum was found for tissue Ca^{2+} compounds, whereas in CCs-containing areas a distinct and specific XAS fingerprint was identified for CPPD crystals.

We first used FT-IR spectroscopy to distinguish cartilage areas with CCs from those without in samples that were initially selected based on the absence of calcifications by macroscopic examination. CCs were present in seven of 12 specimens, from four of six patients, suggesting that FT-IR spectroscopy was sensitive for detecting calcifications in our biological samples. However, FT-IR spectroscopy may have failed to detect calcifications in some of the samples, owing to heterogeneous location of CCs within the OA cartilage.

FT-IR reflects only the overall chemical composition of the species contained in the sample at the molecular scale, including lipids, proteins and PO_4 groups associated with Ca^{2+} (Estepa & Daudon, 1997). Therefore, we also used XANES spectroscopy at the Ca^{2+} *K*-edge to specifically characterize Ca^{2+}-compound-containing species. We found at least two distinct types of Ca^{2+} compounds in OA articular cartilage. One type was found in OA cartilage areas without CCs and seemed to be composed of tissue Ca^{2+} compounds, *i.e.* not linked to mineral compounds, as the XANES spectrum was similar to that found in hydrated tissues. In these areas, tissue Ca^{2+} was the main Ca^{2+} compound, whereas Ca^{2+} involved in CCs was absent or less abundant. The other type of Ca^{2+} compound was identified in CCs-containing OA articular cartilage areas and had an XANES spectrum specific of CPPD crystals. As mentioned above, our sample preparation protocol was suitable for preserving the physico-chemical integrity of the mineral part of the sample. Preservation of tissue ions such as Ca^{2+} may require specific preparation protocols (Boxer *et al.*, 2009).

Despite the technical difficulty in preserving diffusible Ca^{2+} ions, XANES appears suitable for accurately characterizing Ca^{2+} compounds in articular cartilage and provides data that complement those supplied by FT-IR spectroscopy. Since XANES is insensitive to polydispersity (Moonen *et al.*, 1995), it allows an assessment of the relative quantity of Ca^{2+} embedded in the calcifications compared with Ca^{2+} in tissues. That XANES is successful in characterizing Ca^{2+} compounds is closely linked to the ability of XANES to characterize poorly crystallized compounds. Numerous studies based on XAS at the Ca^{2+} *K*-edge have been performed on other biological samples (Carpentier *et al.*, 2010). Thus, XAS has been used to evaluate Ca^{2+} in physiologically calcified tissues such as bones and teeth or apatitic and non-apatitic Ca^{2+} phosphates of biological interest.

5. Conclusion

In summary, in the present study we show that XANES spectroscopy can be used to accurately characterize sparse CCs in human OA cartilage. We find that Ca^{2+} compounds differ between calcified and non-calcified cartilage areas. In calcified areas they appear to be mainly involved in calcifications, namely Ca^{2+} crystals. Further application of synchrotron-radiation-related technologies should bring additional information about other important chemical elements involved in these calcifications.

All the authors are members of the European Crystal Research Network formed after the 1st European Crystal Workshop in Paris on 11–12 March 2010 (convenors: Professor Frédéric Lioté, Paris; and Professor Alexander So, Lausanne). All authors declared no competing of interests. This work was supported by a ANR-09-BLAN-0120-0 contract.

References

Anderson, H. C. (1995). *Clin. Orthop. Relat. Res.* **314**, 266–280.
Bazin, D., Carpentier, X., Brocheriou, I., Dorfmuller, P., Aubert, S., Chappard, C., Thiaudière, D., Reguer, S., Waychunas, G., Jungers, P. & Daudon, M. (2009*b*). *Biochimie*, **91**, 1294–1300.
Bazin, D., Chappard, Ch., Combes, Ch., Carpentier, X., Rouzière, S., André, G., Matzen, G., Allix, M., Thiaudière, D., Reguer, S., Jungers, P. & Daudon, M. (2009*a*). *Osteoporosis Int.* **20**, 1065–1075.
Bazin, D., Chevallier, P., Matzen, G., Jungers, P. & Daudon, M. (2007). *Urol. Res.* **35**, 179–184.
Bazin, D., Daudon, M., Chevallier, P., Rouzière, S., Elkaim, E., Thiaudière, D., Fayard, B., Foy, E., Albouy, P. A., André, G., Matzen, G. & Veron, E. (2006). *Ann. Biol. Clin.* **64**, 125–139.
Bendele, A. M. & Hulman, J. F. (1988). *Arthritis Rheum.* **31**, 561–565.
Bertsch, P. M. & Hunter, D. B. (2001). *Chem. Rev.* **101**, 1809–1842.
Bonen, D. K. & Schmid, T. M. (1991). *J. Cell Biol.* **115**, 1171–1178.
Boxer, S. G., Kraft, M. L. & Weber, P. K. (2009). *Annu. Rev. Biophys.* **38**, 53–74.
Camerlain, M., McCarty, D. J., Silcox, D. C. & Jung, A. (1975). *J. Clin. Invest.* **55**, 1373–1381.
Carpentier, X., Bazin, D., Jungers, P., Reguer, S., Thiaudière, D. & Daudon, M. (2010). *J. Synchrotron Rad.* **17**, 374–379.
Derfus, B. A., Kurian, J. B., Butler, J. J., Daft, L. J., Carrera, G. F., Ryan, L. M. & Rosenthal, A. K. (2002). *J. Rheumatol.* **29**, 570–574.
Dumas, P., Sockalingum, G. D. & Sule-Suso, J. (2006). *Trends Biotechnol.* **25**, 40–44.
Ea, H. K. & Lioté, F. (2009). *Curr. Opin. Rheumatol.* **21**, 150–157.
Ea, H. K., Nguyen, C., Bazin, D., Bianchi, A., Guicheux, J., Reboul, P., Daudon, M. & Lioté, F. (2011). *Arthritis Rheum.* **63**, 10–18.
Eichert, D., Salomé, M., Banu, M., Susini, J. & Rey, C. (2005). *Spectrochim. Acta B*, **60**, 850–858.
Estepa, L. & Daudon, M. (1997). *Biospectroscopy*, **3**, 347–369.
Evans, R. G., Collins, C., Miller, P., Ponsford, F. M. & Elson, C. J. (1994). *Osteoarthritis Cartilage*, **2**, 103–109.
Fam, A. G., Morava-Protzner, I., Purcell, C., Young, B. D., Bunting, P. S. & Lewis, A. J. (1995). *Arthritis Rheum.* **38**, 201–210.
Fuerst, M., Bertrand, J., Lammers, L., Dreier, R., Echtermeyer, F., Nitschke, Y., Rutsch, F., Schäfer, F. K., Niggemeyer, O., Steinhagen, J., Lohmann, C. H., Pap, T. & Rüther, W. (2009). *Arthritis Rheum.* **60**, 2694–2703.
Fuerst, M., Niggemeyer, O., Lammers, L., Schäfer, F., Lohmann, C. & Rüther, W. (2009). *BMC Musculoskelet. Disord.* **10**, 166.
Gigout, A., Jolicoeur, M. & Buschmann, M. D. (2005). *Osteoarthritis Cartilage*, **13**, 1012–1024.
Guinier, A. (1956). *X-ray Diffraction in Crystals, Imperfect Crystals and Amorphous Bodies.* Paris: Dunod.
Hunter, D. J. & Felson, D. T. (2006). *Br. Med. J.* **332**, 639–642.
Johnson, K., Hashimoto, S., Lotz, M., Pritzker, K., Goding, J. & Terkeltaub, R. (2001). *Arthritis Rheum.* **44**, 1071–1081.
Kirsch, T., Swoboda, B. & Nah, H. (2000). *Osteoarthritis Cartilage*, **8**, 294–302.
Kneipp, K., Kneipp, H., Itzkan, I., Dasari, R. R. & Feld, M. S. (1999). *Chem. Rev.* **99**, 2957–2976.
McCarty, D. J., Lehr, J. R. & Halverson, P. B. (1983). *Arthritis Rheum.* **26**, 1220–1224.
McCarthy, G. M. & Cheung, H. S. (2009). *Curr. Rheumatol. Rep.* **11**, 141–147.
McKelvy, M. L., Britt, T. R., Davis, B. L., Gillie, J. K., Graves, F. B. & Lentz, L. A. (1998). *Anal. Chem.* **70**, 119–177.
Mandel, N. & Mandel, G. (1988). *Rheum. Dis. Clin. North Am.* **14**, 321–340.
Moonen, J., Slot, J., Lefferts, L., Bazin, D. & Dexpert, H. (1995). *Physica B*, **208–209**, 689–690.
Nguyen, C., Ea, H. K., Bazin, D., Daudon, M. & Lioté, F. (2010). *Arthritis Rheum.* **62**, 2829–2830.
Pritzker, K. P., Châteauvert, J. M. & Grynpas, M. D. (1987). *J. Rheumatol.* **14**, 806–810.
Sauer, G. R. & Wuthier, R. E. (1988). *J. Biol. Chem.* **263**, 13718–13724.
Scotchford, C. A. & Ali, S. Y. (1995). *Ann. Rheum. Dis.* **54**, 339–344.
Sowrey, F. E., Skipper, L. J., Pickup, D. M., Drake, K. O., Lin, Z., Smith, M. E. & Newport, R. J. (2004). *Phys. Chem. Chem. Phys.* **6**, 188–192.
Terkeltaub, R. A. (2001). *Am. J. Physiol. Cell Physiol.* **281**, C1–C11.
Termine, J. D. & Eanes, E. D. (1974). *Calcif. Tissue Res.* **15**, 81–84.
Yarker, Y. E., Hukins, D. W. & Nave, C. (1984). *Connect. Tissue Res.* **12**, 337–343.
Zoeger, N., Roschger, P., Hofstaetter, J. G., Jokubonis, C., Pepponi, G., Falkenberg, G., Fratzl, P., Berzlanovich, A., Osterode, W., Streli, C. & Wobrauschek, P. (2006). *Osteoarthritis Cartilage*, **14**, 906–913.